

**JAERI - M**  
**93-049**

**SUMMARY REPORT FOR IAEA CRP ON LIFETIME PREDICTION  
FOR THE FIRST WALL OF A FUSION MACHINE  
(JAERI CONTRIBUTION)**

March 1993

Satoshi SUZUKI, Masanori ARAKI and Masato AKIBA

JAERI-Mレポートは、日本原子力研究所が不定期に公刊している研究報告書です。  
入手の問い合わせは、日本原子力研究所技術情報部情報資料課（〒319-11茨城県那珂郡東海村）あて、お申しこしてください。なお、このほかに財団法人原子力弘済会資料センター（〒319-11茨城県那珂郡東海村日本原子力研究所内）で複写による実費頒布をおこなっております。

JAERI-M reports are issued irregularly.

Inquiries about availability of the reports should be addressed to Information Division, Department of Technical Information, Japan Atomic Energy Research Institute, Tokai-mura, Naka-gun, Ibaraki-ken 319-11, Japan.

© Japan Atomic Energy Research Institute, 1993

---

編集兼発行 日本原子力研究所  
印刷 株式会社原子力資料サービス

Summary Report for IAEA CRP on Lifetime Prediction  
for the First Wall of a Fusion Machine  
(JAERI Contribution)

Satoshi SUZUKI, Masanori ARAKI and Masato AKIBA

Department of Fusion Engineering Research  
Naka Fusion Research Establishment  
Japan Atomic Energy Research Institute  
Naka-machi, Naka-gun, Ibaraki-ken

(Received February 9, 1993)

IAEA Coordinated Research Program (CRP) on "Lifetime Prediction for the First Wall of a Fusion Machine" was started in 1989. Five participants, Joint Research Centre (JRC-Ispra), The NET team, Kernforschungszentrum Karlsruhe (KfK), Russian Research Center and Japan Atomic Energy Research Institute, contributed in this activity.

The purpose of the CRP is to evaluate the thermal fatigue behavior of the first wall of a next generation fusion machine by means of numerical methods and also to contribute the design activities for ITER (International Thermonuclear Experimental Reactor). Thermal fatigue experiments of a first wall mock-up which were carried out in JRC-Ispra were selected as a first benchmark exercise model. All participants performed finite element analyses with various analytical codes to predict the lifetime of the simulated first wall. The first benchmark exercise has successfully been finished in 1992. This report summarizes a JAERI's contribution for this first benchmark exercise.

Keywords: IAEA CRP, First Wall, Thermal Fatigue, ITER, Benchmark Exercise, Thermal Stress Analysis

IAEAにおける核融合実験炉第1壁寿命評価研究協力会議のまとめ  
(原研における活動)

日本原子力研究所那珂研究所核融合工学部  
鈴木 哲・荒木 政則・秋葉 真人

(1993年2月9日受理)

1989年、IAEAにおいて「核融合実験炉第1壁の寿命評価」研究協力会議が開始され、イスブラ研究所(JRC-Ispra)、NETチーム、カールスルーエ研究所(KfK)、ロシア研究所(旧クルチャトフ研究所)及び原研の5つの研究所がこの活動に参加した。

本研究協力会議の目的は、次期核融合実験炉の第1壁の熱疲労寿命を数値解析によって予測し、国際熱核融合実験炉(ITER)の設計活動に貢献することである。今回は、イスブラ研究所において実施された第1壁模擬試験体の熱疲労実験がベンチマーク問題のモデルとして採用された。参加者は有限要素解析コードを用いて解析を実施し、模擬試験体の熱疲労寿命を予測した。本解析モデルに対する研究協力会議は1992年に終了した。本報告はこの研究協力会議に対する原研の活動をまとめたものである。

## Contents

|  |   |
|--|---|
| 1. Introduction .....  | 1 |
| 2. Geometry Definitions .....  | 1 |
| 3. Two Dimensional Thermal Analysis .....                                  | 2 |
| 3.1 Mesh for FEM Analyses .....  | 2 |
| 3.2 Analytical Condition .....   | 2 |
| 3.3 Thermal Property .....   | 2 |
| 3.4 Results of the Thermal Analysis .....                                  | 3 |
| 4. Two Dimensional Elastic Thermal Stress Analysis .....                   | 3 |
| 4.1 Boundary Condition .....   | 3 |
| 4.2 Mechanical Property .....  | 3 |
| 4.3 Results of the Elastic Stress Analysis .....                           | 3 |
| 4.4 Evaluation of Fatigue Lifetime .....                                   | 4 |
| 4.4.1 ASME Boiler and Pressure Vessel Code (ASME Code) .....               | 4 |
| 4.4.2 Monju Code (Monju: Japanese Prototype Fast Breeder<br>Reactor) ..... | 5 |
| 5. Two Dimensional Elastic-plastic Thermal Stress Analysis .....           | 6 |
| 5.1 Mechanical Properties .....  | 6 |
| 5.2 Results of the Elastic-plastic Analysis .....                          | 6 |
| 6. Conclusions .....   | 6 |
| Acknowledgement .....  | 8 |
| Reference .....  | 8 |

## 目 次

|                           |   |
|---------------------------|---|
| 1. 序 論 .....              | 1 |
| 2. 試験体の形状 .....           | 1 |
| 3. 2次元熱伝導解析 .....         | 2 |
| 3.1 有限要素解析に使用したメッシュ ..... | 2 |
| 3.2 解析条件 .....            | 2 |
| 3.3 熱物性 .....             | 2 |
| 3.4 熱伝導解析結果 .....         | 3 |
| 4. 2次元弾性応力解析 .....        | 3 |
| 4.1 境界条件 .....            | 3 |
| 4.2 機械的性質 .....           | 3 |
| 4.3 弾性応力解析結果 .....        | 3 |
| 4.4 疲労寿命評価 .....          | 4 |
| 4.4.1 ASMEコード .....       | 4 |
| 4.4.2 もんじゅコード .....       | 5 |
| 5. 2次元弾塑性応力解析 .....       | 6 |
| 5.1 機械的性質 .....           | 6 |
| 5.2 弾塑性応力解析結果 .....       | 6 |
| 6. 結 論 .....              | 6 |
| 謝 辞 .....                 | 8 |
| 参考文献 .....                | 8 |

## 1. INTRODUCTION

The first wall of fusion machines are subjected to a high heat load from the ITER plasma. The heat load is estimated to be 0.2 - 0.6 MW/m<sup>2</sup> in ITER (International Thermonuclear Experimental Reactor). To remove the high heat load from fusion plasma, the actively cooled structure is necessary for the first wall components. The next generation fusion machines, such as ITER, is planned to be operated under pulsed mode. A large number of cyclic thermal loads will be applied to the first wall. The lifetime of the first wall is affected by the cyclic thermal stress due to the pulsed operation. The minimum lifetime of the first wall in ITER is designed to be at least 20,000 thermal cycles. The first wall is also required to withstand against such cyclic heat loads. Since none of the published evaluation methods are available in the lifetime, it is significant to evaluate the lifetime of a first wall by the use of the combination of experimental methods using a small specimen and numerical analyses using finite element codes.

IAEA CRP on "Lifetime Prediction for the First Wall of a Fusion Machines" has proposed to predict the lifetime of first wall structures under cyclic thermal load by numerical analyses and to establish an evaluation method on it. As a first step, numerical analyses predicting the fatigue lifetime of first wall specimen were carried out to compare the results from thermal fatigue experiments on a simulated first wall specimen performed by JRC Ispra. This report presents the evaluation method of fatigue lifetime of the specimen by numerical analyses.

## 2. GEOMETRY DEFINITIONS[1]

Figure 1 shows a geometry of the specimen. The first wall specimen tested is made of an austenitic stainless steel SUS316 (European reactor grade). It has 5 cooling channels of 8 mm inner diameter at a distance of 10 mm from its surface. The specimen is cyclically heated by infrared lamps. The infrared lamps produce almost uniform heat flux on it. The surface of the specimen is coated with chromium and chromium oxide to increase the absorption rate of the infrared from the lamps. As shown in figure 1, the specimen was supported by two arms fixed at both ends of the specimen.

### 3. TWO DIMENSIONAL THERMAL ANALYSIS

#### 3.1. MESH FOR FEM ANALYSES

A thermal analysis has been carried out by the use of 2-dimensional FE mesh. Considering symmetrical geometry of the specimen, 2-dimensional 1/2 model was selected for the analyses. Figure 2-(A) shows the FE mesh in these analyses. It consists of 820 linear elements and 922 nodes in total. Figures 2-(B) and 2-(C) also show the node number and element number at selected points for the evaluation of its lifetime, respectively. All FE analyses were carried out by the use of "ABAQUS ver. 4-8-4" FE code.

#### 3.2. ANALYTICAL CONDITION

In the thermal analysis, following analytical conditions are assumed;

- (1) Uniform heat transfer coefficient at cooling channel is assumed to be a constant value of 9000  $W/m^2 K$ .
- (2) Heat flux of  $0.5 MW/m^2$  is uniformly deposited to the surface of the specimen.
- (3) No radiative cooling effect is considered.
- (4) Coolant temperature is fixed at  $20.0 ^\circ C$  during thermal cycles.
- (5) The constraints by the supporting arms have not been considered.
- (6) The residual stress of the specimen due to manufacturing process have not been considered.

A cyclic thermal load scenario is shown in Fig. 3. Thermal boundary conditions for the analyses are shown in Fig. 4. In the thermal analysis, steady-state heat transfer calculation at the heat flux of  $0.04 MW/m^2$  during preheat condition was performed first. After the calculation, using the temperature distribution of the preheat condition as an initial temperature, the transient thermal analysis was carried out for a thermal cycle.

#### 3.3. THERMAL PROPERTY

The thermal properties of SUS316 stainless steel used in the analyses are summarized in TABLE I. In the present analysis, the thermal properties were considered as a function of temperature except its density; the constant density of  $8000 kg/m^3$  was assumed.



### 3.4. RESULTS OF THE THERMAL ANALYSIS

Since the specimen was preheated at a heat flux of  $0.04 \text{ MW/m}^2$  for a long period, the initial temperature distributions of the specimen for the transient thermal analysis should be regarded as those obtained in the steady-state analysis under preheating condition. Figure 5 shows the temperature distributions under the preheat condition. The initial temperature values of the selected points are summarized in TABLE II.

Thermal load scenario shown in Fig. 3 was applied to the model. The results of transient thermal analysis are summarized as follows;

The maximum temperature of  $451.7 \text{ }^\circ\text{C}$  appears at the point H (Node number 271) at the end of heating period. A base temperature of point H is expected to increase from initial temperature of  $60.52 \text{ }^\circ\text{C}$  to  $107.6 \text{ }^\circ\text{C}$ . To reach steady-state temperature condition, it is expected to take several thermal cycles. Thermal responses at the selected points are shown in Fig. 6-(A)-(E), respectively.

## 4. TWO DIMENSIONAL ELASTIC THERMAL STRESS ANALYSIS

The elastic thermal stress analysis has been performed to predict the lifetime of the specimen by referring from ASME code section III NB[2] and Monju code[3]. In this analysis, generalized plane strain elements was selected for the aim of simulating 3-dimensional effect of the model.

### 4.1. BOUNDARY CONDITION

Mechanical boundary conditions for the elastic analysis are described in Fig. 7. Nodes on the center line was constrained along X-direction. Out-of-plane (along Z-direction) bending was constrained in this model.

### 4.2. MECHANICAL PROPERTY

The mechanical properties of SUS316 stainless steel used in the stress analysis are shown in TABLE III. In this analyses, they are also considered as a function of a temperature.

### 4.3. RESULTS OF THE ELASTIC STRESS ANALYSIS

Mises equivalent stress contours at the conditions under preheating and the end of heating are

shown in Fig. 8 and Fig. 9, respectively. TABLES IV and V also summarize minimum principal stress, maximum principal stress, Mises equivalent stress, Tresca equivalent stress and Mises equivalent strain range ( $\Delta\epsilon$  eq.) at the conditions under preheating and the end of heating.

Maximum principal stress of 721.9 MPa is estimated in the Element No. 292 at the end of heating; minimum principal stress is almost 0 MPa in Element No. 41 at the preheat condition. Maximum Mises equivalent stress value of 986.7 MPa at the edge of specimen surface ( i.e. Element No. 233 including point H ) was expected. Maximum Mises equivalent strain range ( $\Delta\epsilon$  eq.) reached to 0.56% at Element No. 233.

#### 4.4. EVALUATION OF FATIGUE LIFETIME

##### 4.4.1. ASME Boiler and Pressure Vessel code (ASME code)

In ASME code sec. III NB, an evaluation of fatigue lifetime for various materials is based on an elastic stress analysis. For the use of this code, all stress values should be classified, such as general primary membrane stress, primary bending stress, secondary peak stress and so on. Based on these stress invariants, stress intensity is calculated. However, in FE analyses, obtained stress values show total stress values. It is difficult to classify these value. Therefore, the stress values obtained in the present analyses were assumed to be secondary bending stresses.

Figure 10 shows a design fatigue curve for stainless steels. This curve includes safety factors. In particular, in a low cycle fatigue region ( $<10^4$  cycles), the fatigue lifetime of this curve includes a safety factor of 20. The realistic fatigue lifetime, that is, the experimental fatigue lifetime, is estimated to be 20 times longer than this curve.

In ASME code section III, Tresca equivalent stress value is required for a conservative prediction of lifetime of the specimen. Maximum Tresca equivalent stress value of 1052 MPa is expected in the Element No. 1 at the end of heating. Young's modulus of AISI316 stainless steel, 194 GPa, is used in this evaluation. As a result, a stress intensity in ASME code section III NB, S, was expected as follows;

$$S = 805 \text{ MPa.}$$

Therefore, the design fatigue curve of ASME code section III ( see Fig. 10 ) gives the minimum fatigue lifetime of around 16,000 cycles at the specimen surface.

#### 4.4.2. Monju code ( Monju : Japanese prototype fast breeder reactor)

Monju code was developed as an analysis and design code for structure materials of FBR with liquid metal cooling system in 1984. Applicable materials of Monju code are mainly chrome-molybdenum steels and austenitic stainless steels (SUS304, SUS316 and SUS321) at an elevated temperature condition. The Monju code is based on ASME Boiler and Pressure Vessel Code section III and its code case N-47. Therefore, the basic concept of the code is also "Design by Analysis". Linear and non-linear analyses are applied for the design of the components.

The descriptions of "Limits to primary stress", "Limits to special stress" and "Limits to buckling" in the Monju code are similar to those in the ASME code case N-47. Linear analyses are used for the consideration of the limits described above. In the Monju code, stresses are distinguished into two kinds. One is "long term stresses", the other is "short term stresses". The long term stresses are the stresses which creep effects can be considered.

Comparing to the ASME code case N-47, the Monju code has characteristics as follows:

The Monju code

- 1) has limits in the case of lower local primary stresses are low.
- 2) does not have a limit to a local stress.
- 3) gives a reasonable limits by considering short term primary stresses (which are separated into several kinds) in the evaluation of an enhanced creep strain.
- 4) has definite limits to secondary stresses (except for the thermal stresses induced by the temperature gradient through a wall thickness direction) by considerations of elastic follow-up.

As described before, the maximum Mises equivalent strain range was calculated to 0.56% in the elastic analysis. According to this value, the lifetime of the specimen can be estimated to be about 80,000 cycles by the Monju code. (See Fig.11)

## 5. TWO DIMENSIONAL ELASTIC-PLASTIC THERMAL STRESS ANALYSIS

To evaluate the fatigue lifetime of the specimen by the use of experimental fatigue life data, 2-dimensional elastic-plastic thermal stress analysis was also performed. In the analysis, only one thermal cycle was applied to the model. Analytical model and boundary conditions are same as those in the elastic analysis.

### 5.1. MECHANICAL PROPERTIES

It was assumed that a stress-strain behavior of AISI316 stainless steel can be approximated to a bi-linear curve as shown in Fig.12. The stress-strain data are based on those of RCC-MR code[4]. Material properties such as Young's modulus, thermal expansion and plastic coefficient were used as a function of a temperature. Since only one thermal cycle was applied to the model, cyclic hardening of the material was not considered in this analysis.

### 5.2. RESULTS OF THE ELASTIC-PLASTIC ANALYSIS

Figure 13 shows a Mises equivalent stress contour at the end of heating. Time histories of Mises equivalent strain range at the selected elements are also shown in Fig.14. Maximum Mises equivalent strain range reached to 0.602 % at the center of the specimen surface (Element No. 1) at the end of heating. Figures 15-(A),(B) shows the history of principal stresses at selected elements.

According to the experimental fatigue life data (see Fig. 16), it is estimated that the fatigue lifetime of the specimen is 1,000~2,000 cycles.

## 6. CONCLUSIONS

- 1) In the elastic analysis, the lifetime of the specimen was estimated to be 16,000 cycles by ASME code.
- 2) On the basis of Monju code, the lifetime was estimated to be 80,000 cycles.
- 3) In the elastic-plastic analysis, the lifetime of the specimen was estimated to be 1,000~2,000 cycles by referring to the experimental fatigue data (uniaxial tensile-compress test) of SUS316 stainless steel.

In the elastic analysis, the difference of each other is much attributable to the different evaluation codes. In ASME code, a lifetime is determined by an allowable stress intensity (S). While, in Monju code, it is determined by an allowable strain range. Moreover, Monju code required to be applied under some limitations. Because of the reasons described above, the design fatigue curve of Monju code is different from that of ASME code. In this way, the lifetime predicted by ASME code is different from the lifetime evaluated by Monju code.

In the elastic-plastic analysis, the estimated lifetime is rather less than those of elastic analysis. The calculated Mises equivalent strain values can be overestimated one because only one thermal cycle was applied to the model. Since the experimental fatigue data used in the evaluation were obtained by uniaxial tensile-compressive fatigue tests, the difference of loading patterns, bending and uniaxial tensile-compressive, will affect the evaluation of the lifetime.

## ACKNOWLEDGEMENT

The authors would like to thank Dr. Ohara and the members of NBI Heating laboratory for enlightening discussions. We would also like to acknowledge Drs. S. Shimamoto and N. Shikazono for their support and encouragement.

## REFERENCE

- [1] MATERA, R., et. al., "Behavior of First Wall Components under Thermal Fatigue", Fusion Technology and Safety, Technical Note No. 1.90.20, Joint Research Centre, (1990)
- [2] ASME Boiler and pressure vessel code, Section III, United Energy Center.
- [3] IIDA, K., et. al., "Simplified analysis and design for elevated temperature components of Monju", Nuclear Engineering and Design vol.98 (1987), 305-317
- [4] RCC-MR, Règles de conception et de construction des matériels mécaniques des îlots nucléaires, Technical Annex A3.1S, A.F.C.E.N., (1985)

TABLE I. THERMAL PROPERTIES OF AISI316 STAINLESS STEEL

| Temp. (°C) | Thermal cond. (W/m K) | Specific heat (J/kg K) |
|------------|-----------------------|------------------------|
| 20.0       | 14.5                  | 480.0                  |
| 300.0      | 18.0                  | 550.0                  |
| 500.0      | 20.0                  | 580.0                  |
| 700.0      | 23.0                  | 600.0                  |

TABLE II. INITIAL TEMPERATURES AT THE SELECTED POINTS

| node No.   | 1     | 5     | 9     | 281   | 338   | 336   | 557   | 562   |
|------------|-------|-------|-------|-------|-------|-------|-------|-------|
| Point name | F&M   |       |       | D     | C     |       |       | A     |
| Temp.(°C)  | 54.81 | 43.96 | 32.51 | 25.96 | 20.34 | 20.65 | 21.39 | 21.53 |

| node No.   | 46    | 50    | 54    | 420   | 351   | 617   | 622   | 271   |
|------------|-------|-------|-------|-------|-------|-------|-------|-------|
| Point name | G     |       |       |       |       |       | B     | H     |
| Temp.(°C)  | 54.93 | 42.85 | 31.29 | 22.58 | 20.96 | 21.44 | 21.58 | 60.52 |

TABLE III. MECHANICAL PROPERTIES OF AISI316 STAINLESS STEEL

| Temp. (°C) | Young's Modulus (GPa) | Thermal Expansion (/K) |
|------------|-----------------------|------------------------|
| 20.0       | 195.0                 | 1.6E-5                 |
| 300.0      | 175.0                 | 1.7E-5                 |
| 500.0      | 155.0                 | 1.8E-5                 |
| 700.0      | 140.0                 | 1.9E-5                 |

TABLE IV . MINIMUM AND MAXIMUM VALUE OF EQUIVALENT STRESSES AT PREHEATING CONDITION

|                                |                        |
|--------------------------------|------------------------|
| minimum principal stress (MPa) | 0.074 (at element 41)  |
| maximum principal stress (MPa) | 63.97 (at element 292) |
| minimum Mises stress (MPa)     | 16.05 (at element 357) |
| maximum Mises stress (MPa)     | 97.73 (at element 233) |
| minimum Tresca stress (MPa)    | 18.27 (at element 357) |
| maximum Tresca stress (MPa)    | 99.95 (at element 233) |

TABLE V . MINIMUM AND MAXIMUM VALUE OF EQUIVALENT STRESSES AT THE END OF HEATING

|                                |                     |
|--------------------------------|---------------------|
| minimum principal stress (MPa) | 0.976 (Element 41)  |
| maximum principal stress (MPa) | 721.9 (Element 292) |
| minimum Mises stress (MPa)     | 159.0 (Element 357) |
| maximum Mises stress (MPa)     | 986.7 (Element 233) |
| minimum Tresca stress (MPa)    | 175.4 (Element 357) |
| maximum Tresca stress (MPa)    | 1052.0 (Element 1)  |



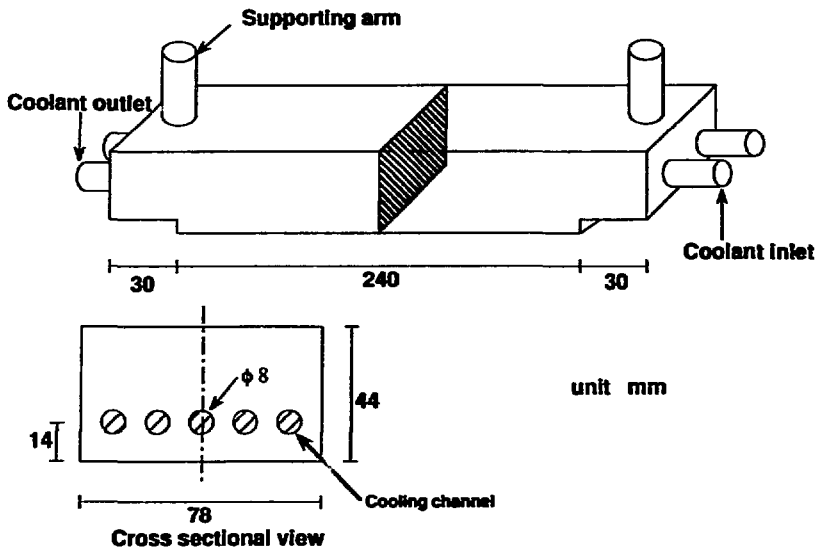


Fig.1 Schematic View of Specimen

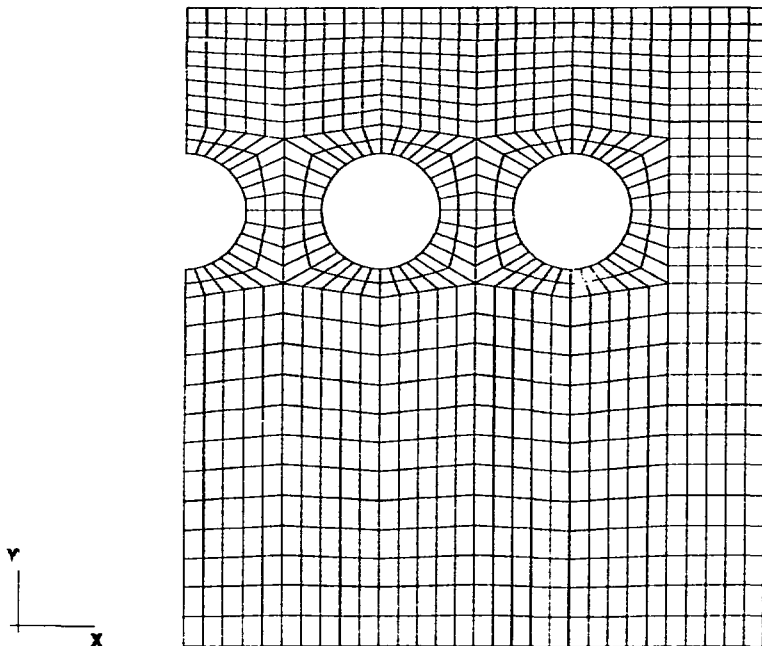


Fig.2-(A) FE Mesh used in the analysis

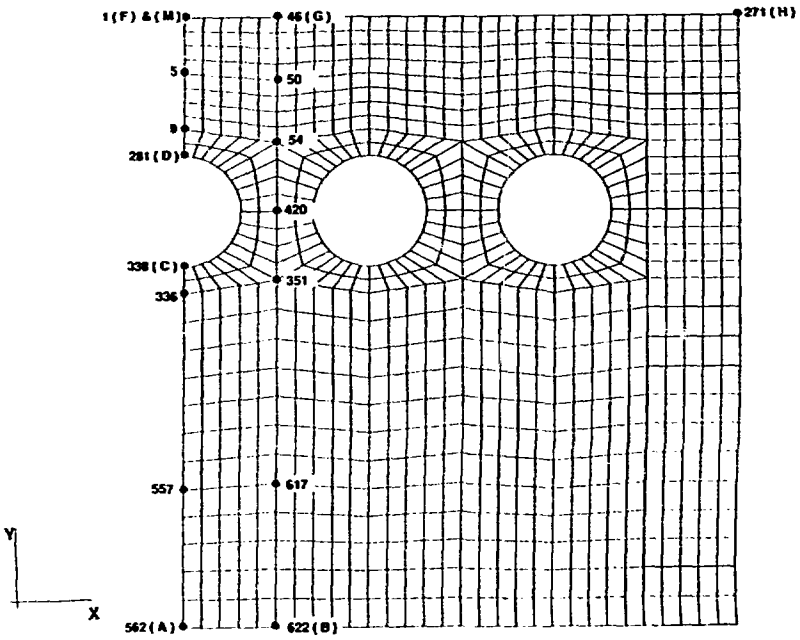


Fig.2-(B) Node Numbering of FE Mesh

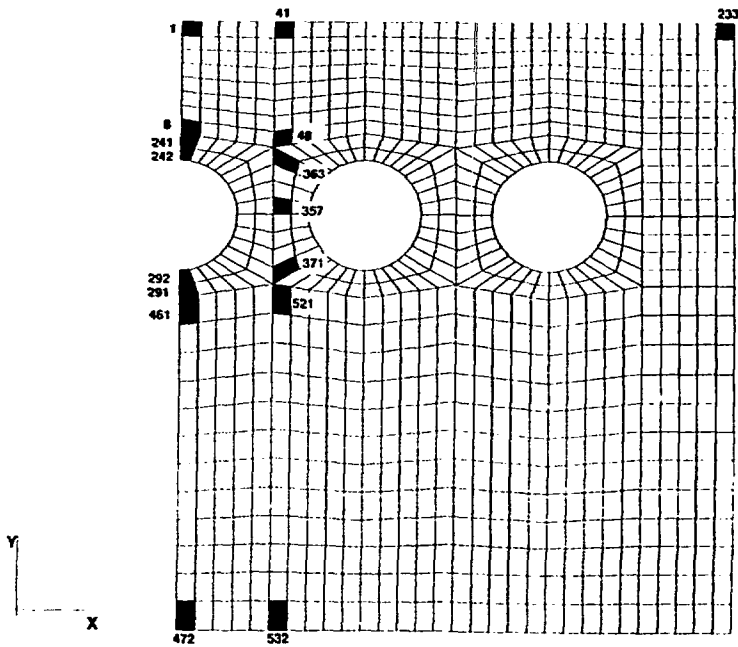


Fig.2-(C) Element Numbering of FE Mesh



at the preheating period

TEMPERATURE (°C)

|    |      |
|----|------|
| 1  | 20.0 |
| 2  | 24.0 |
| 3  | 28.0 |
| 4  | 32.0 |
| 5  | 36.0 |
| 6  | 40.0 |
| 7  | 44.0 |
| 8  | 48.0 |
| 9  | 52.0 |
| 10 | 56.0 |
| 11 | 60.0 |

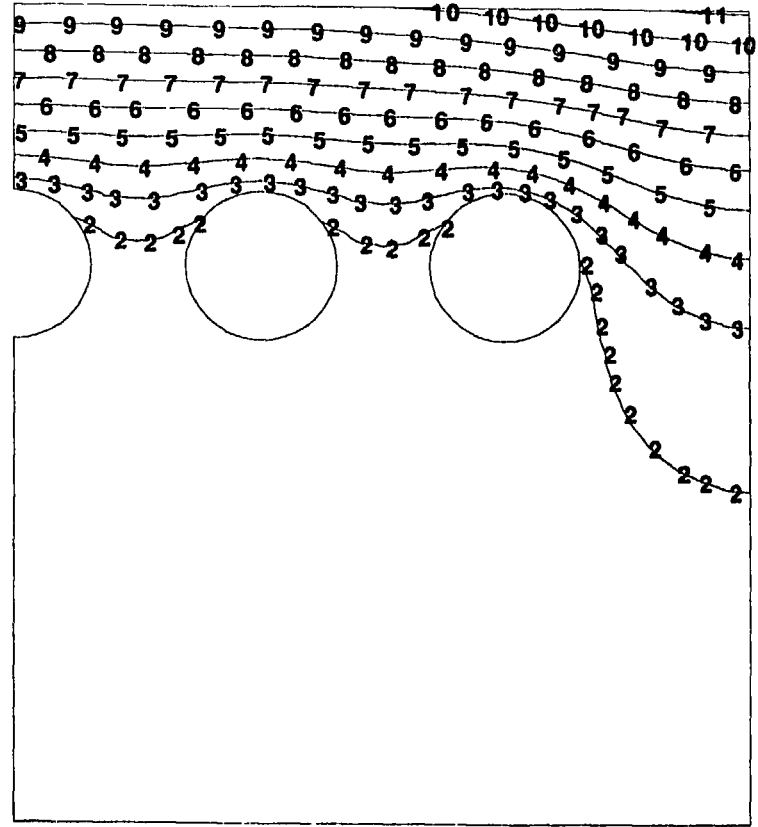
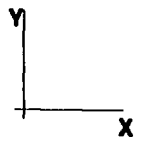


Fig.5 Temperature Distribution at Preheat Condition (Steady-State Analysis)

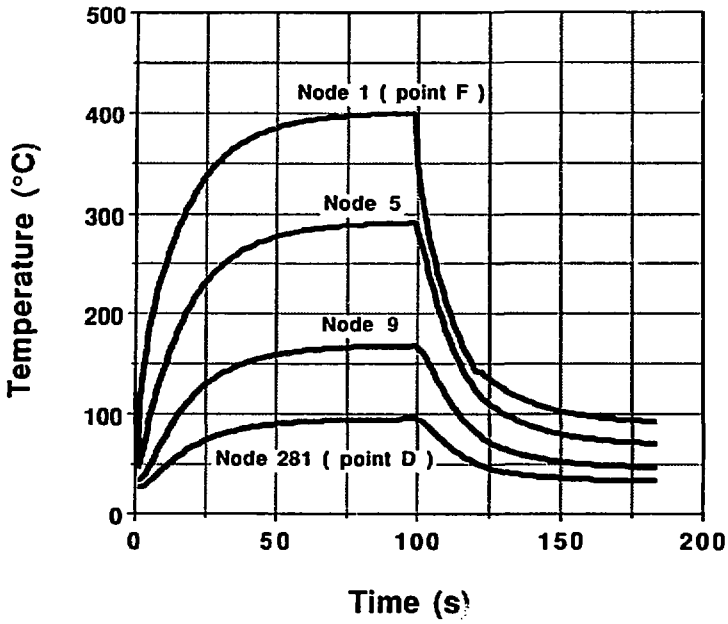


Fig.6-(A) Time history of temperature along DF line

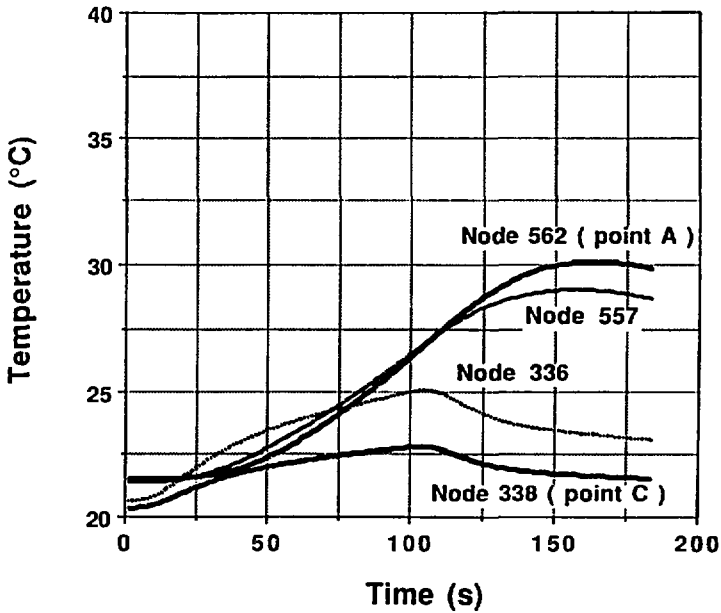


Fig.6-(B) Time history of temperature along AC line

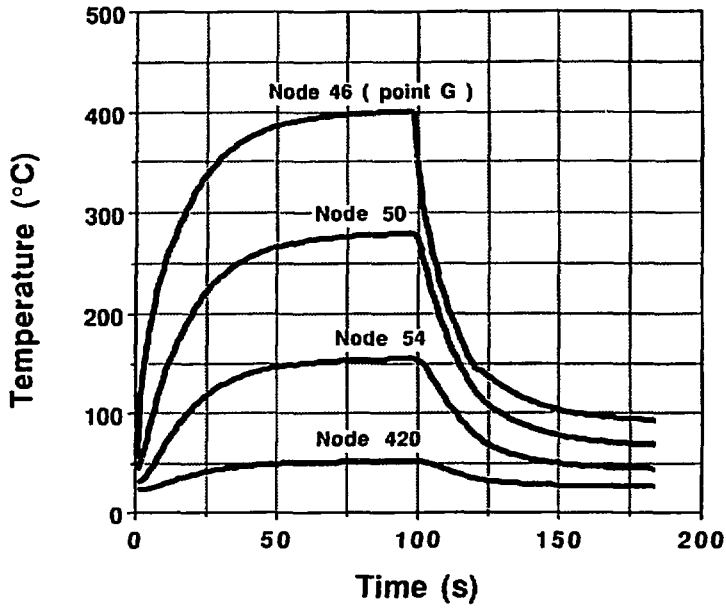


Fig.6-(C) Time history of temperature along BG line

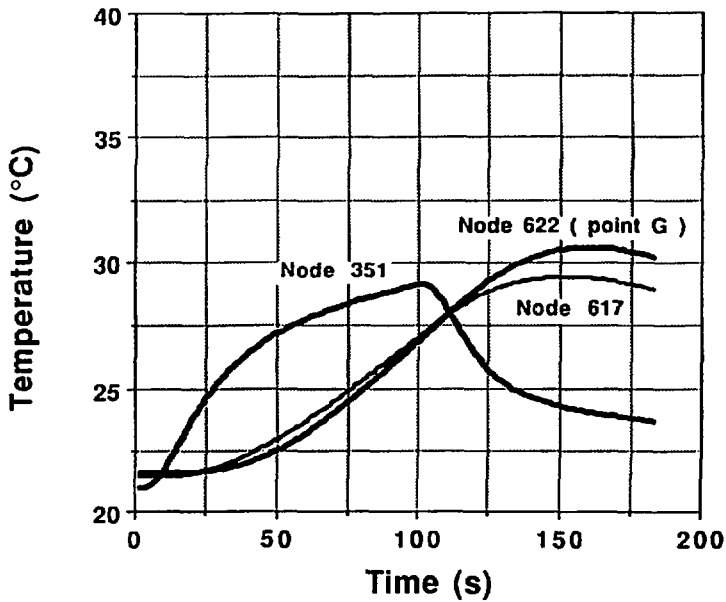


Fig.6-(D) Time history of temperature along BG line

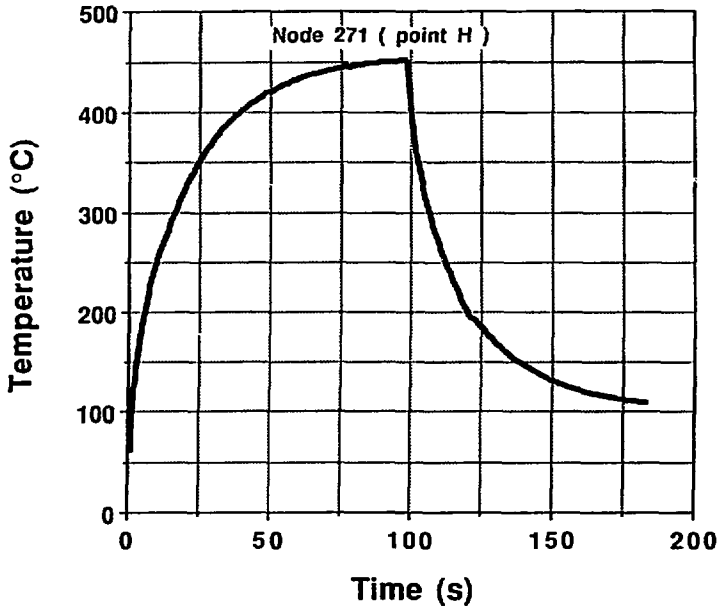


Fig.6-(E) Time history of temperature of point H

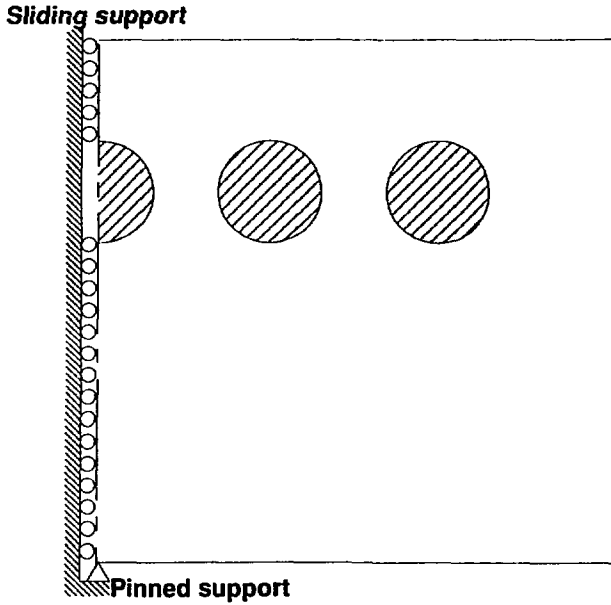


Fig.7 Mechanical Boundary Condition

at the preheating period

MISES VALUE ( MPa )

|    |       |
|----|-------|
| 1  | 10.0  |
| 2  | 19.0  |
| 3  | 28.0  |
| 4  | 37.0  |
| 5  | 46.0  |
| 6  | 55.0  |
| 7  | 64.0  |
| 8  | 73.0  |
| 9  | 82.0  |
| 10 | 91.0  |
| 11 | 100.0 |

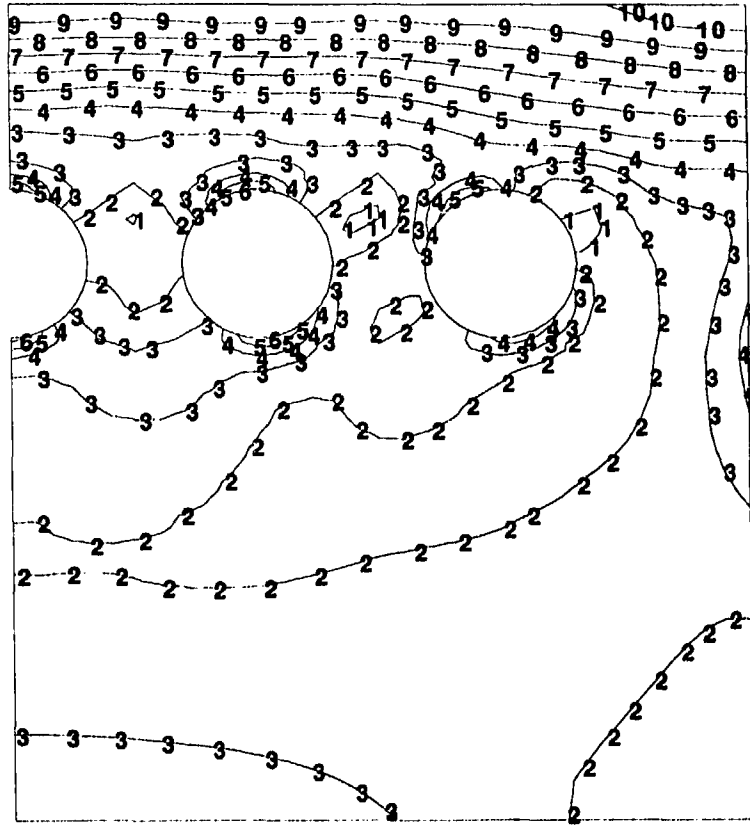
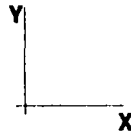


Fig.8 Mises Stress Contour(Elastic Thermal Stress Analysis)



at the end of heating

MISES VALUE ( MPa )

|    |        |
|----|--------|
| 2  | 190.0  |
| 3  | 280.0  |
| 4  | 370.0  |
| 5  | 460.0  |
| 6  | 550.0  |
| 7  | 640.0  |
| 8  | 730.0  |
| 9  | 820.0  |
| 10 | 910.0  |
| 11 | 1000.0 |

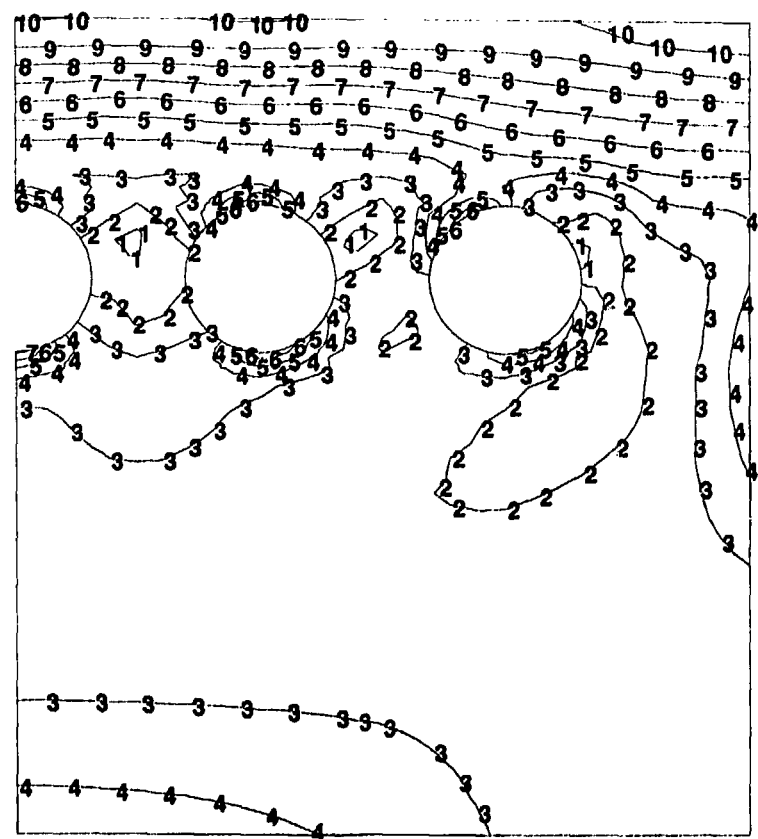
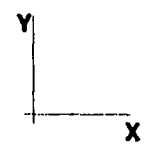


Fig.9 Mises Stress Contour(Elastic Thermal Stress Analysis)

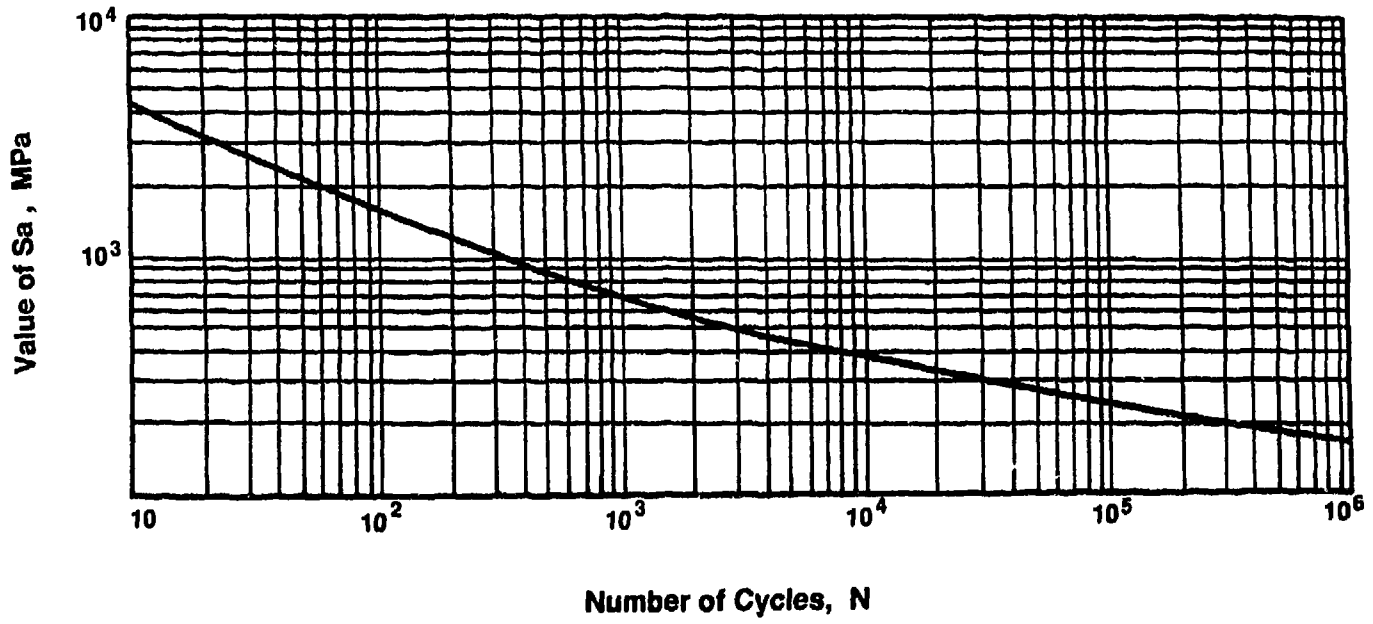


Fig.10 Design Fatigue Curve for Austenitic Stainless Steels

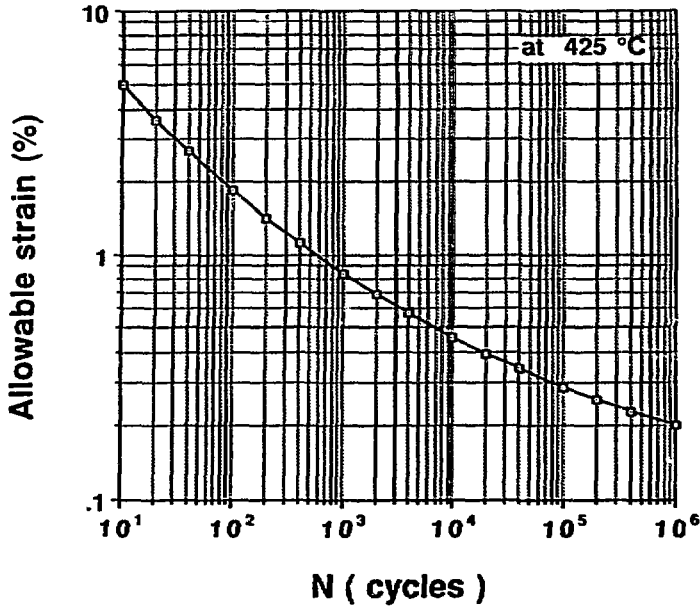
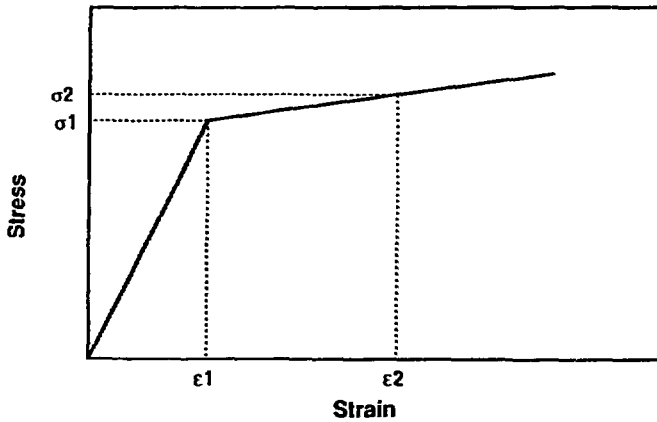


Fig.11 Design fatigue curve of Monju code



|       | $\epsilon 1(\%)$ | $\sigma 1(\text{MPa})$ | $\epsilon 2(\%)$ | $\sigma 2(\text{MPa})$ | $E(\text{GPa})$ |
|-------|------------------|------------------------|------------------|------------------------|-----------------|
| 20°C  | 0.117            | 206.13                 | 0.449            | 285.73                 | 195             |
| 300°C | 0.0832           | 124.46                 | 0.401            | 172.52                 | 175             |
| 500°C | 0.0607           | 108.22                 | 0.398            | 150.01                 | 155             |

Fig.12 Bi-linear data for kinematic hardening

at the end of heating

MISES VALUE ( MPa )

|    |       |
|----|-------|
| 2  | 30.0  |
| 3  | 60.0  |
| 4  | 90.0  |
| 5  | 120.0 |
| 6  | 150.0 |
| 7  | 180.0 |
| 8  | 210.0 |
| 9  | 240.0 |
| 10 | 270.0 |
| 11 | 300.0 |

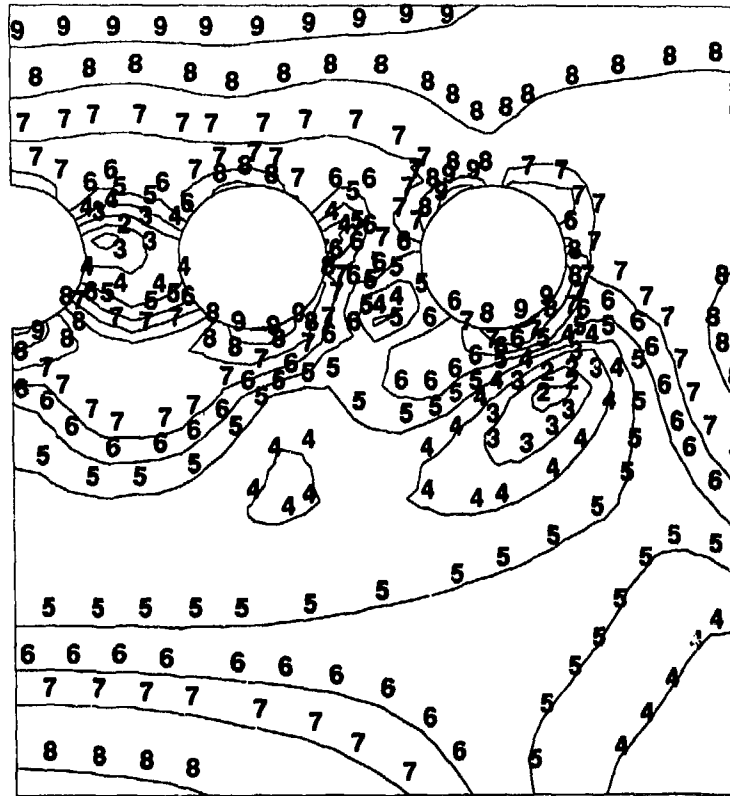
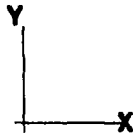


Fig.13 Mises Stress Contour (Elastic-Plastic Thermal Stress Analysis)

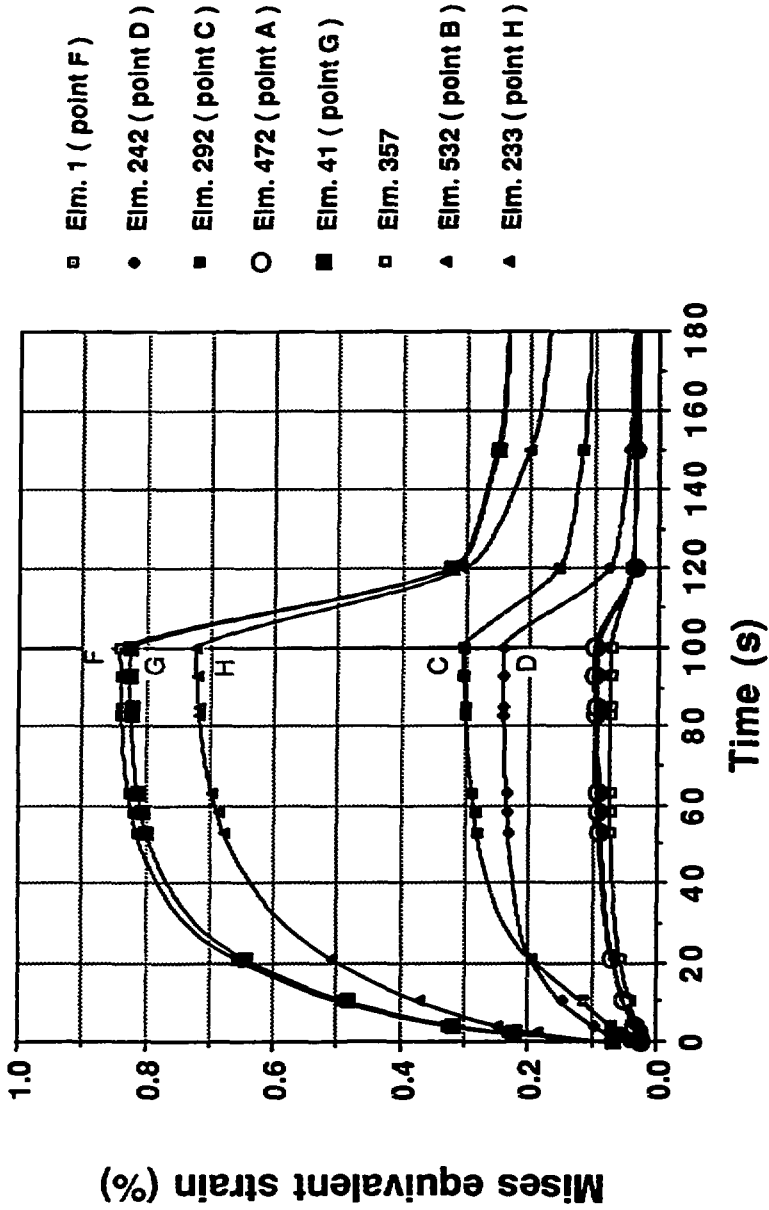


Fig.14 Time history of Mises equivalent strain at selected points

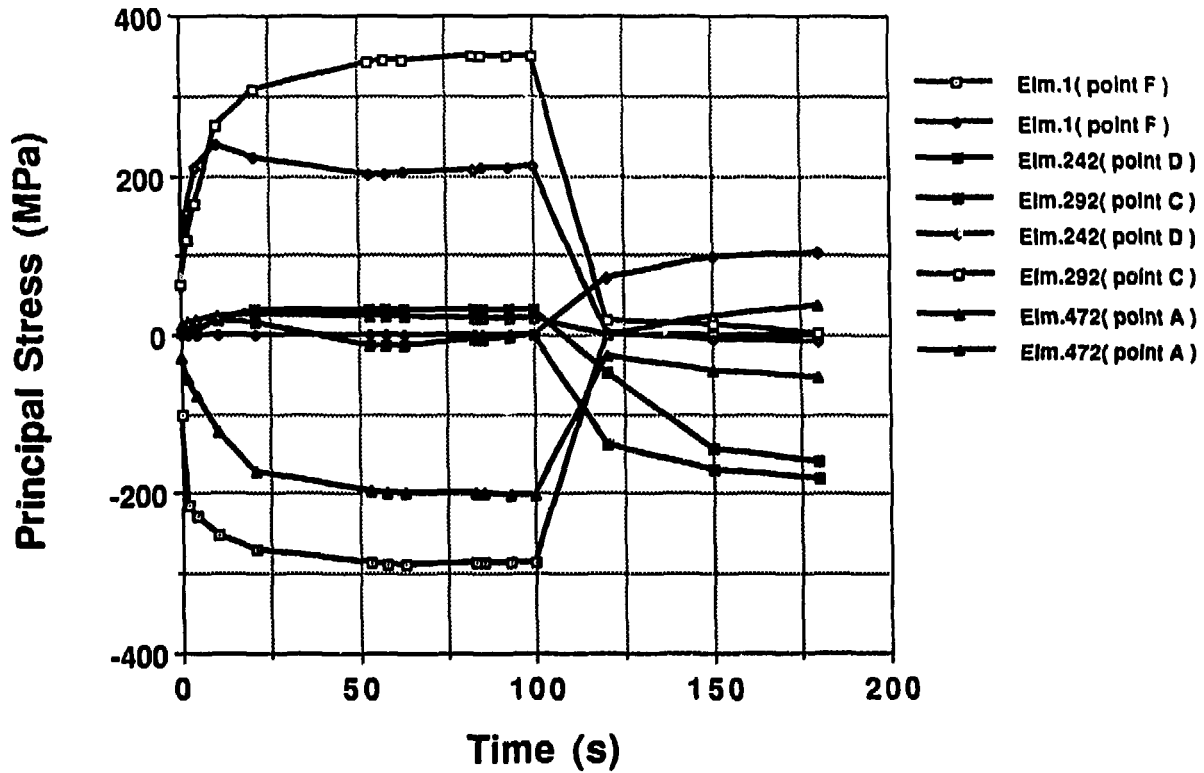


Fig.15-(A) Maximum and minimum principal stresses along AC AND DF line

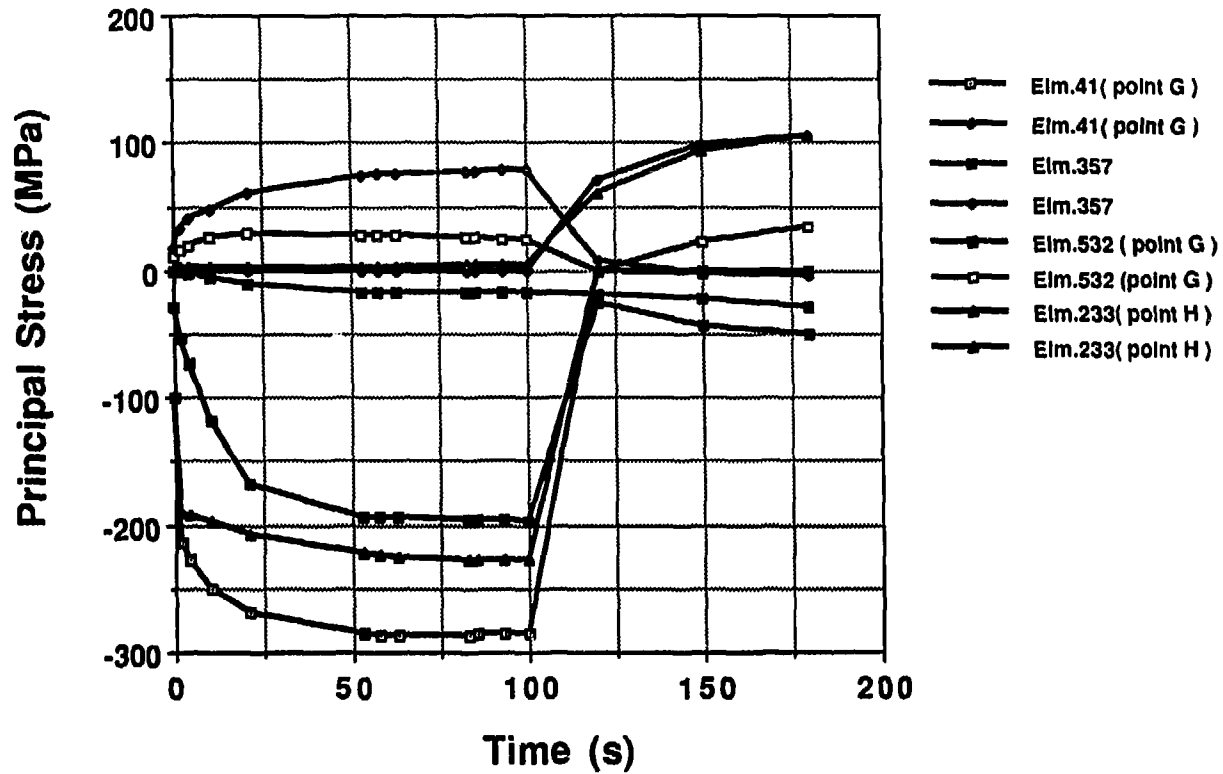


Fig.15-(B) Maximum and minimum principal stress along BG line and point H

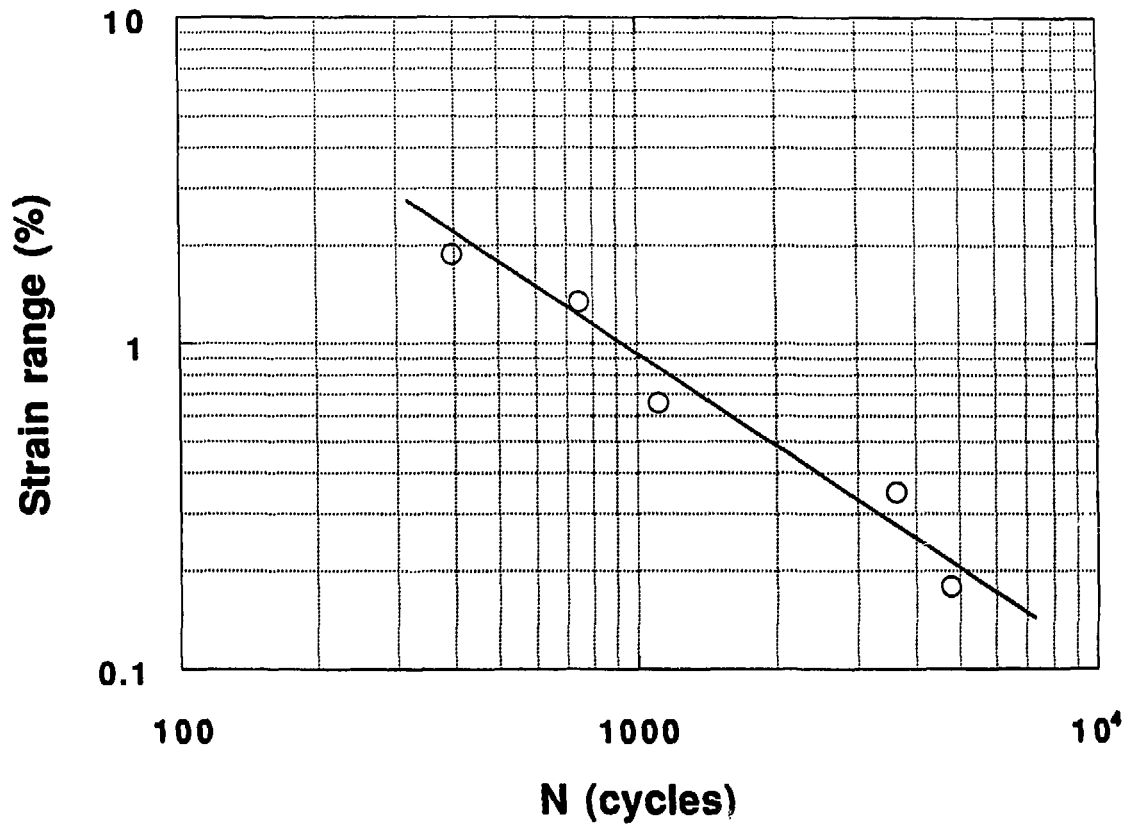


Fig.16 Experimental fatigue data



# 国際単位系 (SI) と換算表

表1 SI基本単位および補助単位

| 量     | 名称     | 記号  |
|-------|--------|-----|
| 長さ    | メートル   | m   |
| 質量    | キログラム  | kg  |
| 時間    | 秒      | s   |
| 電流    | アンペア   | A   |
| 熱力学温度 | ケルビン   | K   |
| 物質の量  | モル     | mol |
| 光度    | カンデラ   | cd  |
| 平面角   | ラジアン   | rad |
| 立体角   | ステラジアン | sr  |

表3 固有の名称をもつSI相対単位

| 量           | 名称     | 記号 | 他のSI単位による表現         |
|-------------|--------|----|---------------------|
| 周波数         | ヘルツ    | Hz | s <sup>-1</sup>     |
| 力           | ニュートン  | N  | m·kg/s <sup>2</sup> |
| 圧力、応力       | パスカル   | Pa | N/m <sup>2</sup>    |
| エネルギー、仕事、熱量 | ジュール   | J  | N·m                 |
| 仕事率、放射束     | ワット    | W  | J/s                 |
| 電気量、電荷      | クーロン   | C  | A·s                 |
| 電位、電圧、起電力   | ボルト    | V  | W/A                 |
| 静電容量        | ファラド   | F  | C/V                 |
| 電気抵抗        | オーム    | Ω  | V/A                 |
| コンダクタンス     | ジーメンズ  | S  | A/V                 |
| 磁束          | ウェーバ   | Wb | V·s                 |
| 磁束密度        | テスラ    | T  | Wb/m <sup>2</sup>   |
| インダクタンス     | ヘンリー   | H  | Wb/A                |
| セルシウス温度     | セルシウス度 | °C |                     |
| 光強度         | ルーメン   | lm | cd·sr               |
| 照度          | ルクス    | lx | lm/m <sup>2</sup>   |
| 放射能         | ヘクレル   | Bq | s <sup>-1</sup>     |
| 吸収線量        | グレイ    | Gy | J/kg                |
| 線量当量        | シーベルト  | Sv | J/kg                |

表2 SIと併用される単位

| 名称     | 記号        |
|--------|-----------|
| 分、時、日  | min, h, d |
| 度、分、秒  | °, ', "   |
| リットル   | l, L      |
| トン     | t         |
| 電子ボルト  | eV        |
| 原子質量単位 | u         |

1 eV = 1.60218 × 10<sup>-19</sup> J  
1 u = 1.66054 × 10<sup>-27</sup> kg

表4 SIと共に暫定的に維持される単位

| 名称       | 記号  |
|----------|-----|
| オングストローム | Å   |
| バー       | bar |
| ガリ       | Gal |
| キュリー     | Ci  |
| レントゲン    | R   |
| ラド       | rad |
| レム       | rem |

1 Å = 0.1 nm = 10<sup>-10</sup> m  
1 b = 100 fm<sup>2</sup> = 10<sup>-28</sup> m<sup>2</sup>  
1 bar = 0.1 MPa = 10<sup>5</sup> Pa  
1 Gal = 1 cm/s<sup>2</sup> = 10<sup>-2</sup> m/s<sup>2</sup>  
1 Ci = 3.7 × 10<sup>10</sup> Bq  
1 R = 2.58 × 10<sup>-4</sup> C/kg  
1 rad = 1 cGy = 10<sup>-2</sup> Gy  
1 rem = 1 cSv = 10<sup>-2</sup> Sv

表5 SI接頭語

| 倍数                | 接頭語  | 記号 |
|-------------------|------|----|
| 10 <sup>18</sup>  | エクサ  | E  |
| 10 <sup>15</sup>  | ペタ   | P  |
| 10 <sup>12</sup>  | テラ   | T  |
| 10 <sup>9</sup>   | ギガ   | G  |
| 10 <sup>6</sup>   | メガ   | M  |
| 10 <sup>3</sup>   | キロ   | k  |
| 10 <sup>2</sup>   | ヘクト  | h  |
| 10 <sup>1</sup>   | デカ   | da |
| 10 <sup>-1</sup>  | デシ   | d  |
| 10 <sup>-2</sup>  | センチ  | c  |
| 10 <sup>-3</sup>  | ミリ   | m  |
| 10 <sup>-6</sup>  | マイクロ | μ  |
| 10 <sup>-9</sup>  | ナノ   | n  |
| 10 <sup>-12</sup> | ピコ   | p  |
| 10 <sup>-15</sup> | フェムト | f  |
| 10 <sup>-18</sup> | アト   | a  |

(注)

- 表1 5は「国際単位系」第5版、国際度量衡局 1985年刊行による。ただし、1 eV および 1 u の値は CODATA の 1986年推奨値によった。
- 表4には海里、ノット、アール、ヘクタールも含まれているが日常の単位なのでここでは省略した。
- bar は、JISでは流体の圧力を表す場合に限り表2のカテゴリに分類されている。
- EC 閣僚理事会指令では bar、barn および「血圧の単位」mmHg を表2のカテゴリに入れている。

## 換算表

| 力       | N (=10 <sup>5</sup> dyn) | kgf      | lbf      |
|---------|--------------------------|----------|----------|
| 1       | 1                        | 0.101972 | 0.224809 |
| 9.80665 |                          | 1        | 2.20462  |
| 4.44822 |                          | 0.453592 | 1        |

粘度 1 Pa·s (= N·s/m<sup>2</sup>) = 10 P (ポアズ) (g/(cm·s))

動粘度 1 m<sup>2</sup>/s = 10<sup>6</sup> St (ストークス) (cm<sup>2</sup>/s)

| 圧                          | MPa (= 10 bar) | kgf/cm <sup>2</sup>        | atm                        | mmHg (Torr)               | lbf/in <sup>2</sup> (psi)  |
|----------------------------|----------------|----------------------------|----------------------------|---------------------------|----------------------------|
| 1                          | 1              | 10.1972                    | 9.86923                    | 7.50062 × 10 <sup>1</sup> | 145.038                    |
| 0.0980665                  |                | 1                          | 0.967841                   | 735.559                   | 14.2233                    |
| 0.101325                   |                | 1.03323                    | 1                          | 760                       | 14.6959                    |
| 1.33322 × 10 <sup>-6</sup> |                | 1.35951 × 10 <sup>-3</sup> | 1.31579 × 10 <sup>-3</sup> | 1                         | 1.93368 × 10 <sup>-2</sup> |
| 6.89476 × 10 <sup>-1</sup> |                | 7.03070 × 10 <sup>-2</sup> | 6.80460 × 10 <sup>-2</sup> | 51.7149                   | 1                          |

| エネルギー・仕事・熱量                 | J (=10 <sup>7</sup> erg) | kgf·m                       | kW·h                        | cal (計量法)                   | Btu                         | ft·lbf                      | eV                         | 1 cal = 4.18605 J (計量法) |
|-----------------------------|--------------------------|-----------------------------|-----------------------------|-----------------------------|-----------------------------|-----------------------------|----------------------------|-------------------------|
| 1                           | 1                        | 0.101972                    | 2.77778 × 10 <sup>-7</sup>  | 0.238889                    | 9.47813 × 10 <sup>-8</sup>  | 0.737562                    | 6.24150 × 10 <sup>18</sup> | = 4.184 J (熱化学)         |
| 9.80665                     |                          | 1                           | 2.72407 × 10 <sup>-6</sup>  | 2.34270                     | 9.29487 × 10 <sup>-3</sup>  | 7.23301                     | 6.12082 × 10 <sup>18</sup> | = 4.1855 J (15 °C)      |
| 3.6 × 10 <sup>6</sup>       |                          | 3.67098 × 10 <sup>5</sup>   | 1                           | 8.59999 × 10 <sup>5</sup>   | 3412.13                     | 2.6122 × 10 <sup>6</sup>    | 2.24694 × 10 <sup>25</sup> | = 4.1868 J (国際蒸気表)      |
| 4.18605                     |                          | 0.426858                    | 1.16279 × 10 <sup>-6</sup>  | 1                           | 3.96759 × 10 <sup>-1</sup>  | 3.08747                     | 2.61272 × 10 <sup>18</sup> | 仕事率 1 PS (仏馬力)          |
| 1055.06                     |                          | 107.586                     | 2.93072 × 10 <sup>-4</sup>  | 252.042                     | 1                           | 778.172                     | 6.58515 × 10 <sup>21</sup> | = 75 kgf·m/s            |
| 1.35582                     |                          | 0.138255                    | 3.76616 × 10 <sup>-7</sup>  | 0.323890                    | 1.28506 × 10 <sup>-3</sup>  | 1                           | 8.46233 × 10 <sup>18</sup> | = 735.499 W             |
| 1.60218 × 10 <sup>-19</sup> |                          | 1.63377 × 10 <sup>-20</sup> | 4.45050 × 10 <sup>-26</sup> | 3.82743 × 10 <sup>-20</sup> | 1.51857 × 10 <sup>-22</sup> | 1.18171 × 10 <sup>-19</sup> | 1                          |                         |

| 放射能                    | Bq | Ci                          |
|------------------------|----|-----------------------------|
| 1                      | 1  | 2.70270 × 10 <sup>-11</sup> |
| 3.7 × 10 <sup>10</sup> |    | 1                           |

| 吸収線量 | Gy | rad |
|------|----|-----|
| 1    | 1  | 100 |
| 0.01 |    | 1   |

| 照射線量                    | C/kg | R    |
|-------------------------|------|------|
| 1                       | 1    | 3876 |
| 2.58 × 10 <sup>-4</sup> |      | 1    |

| 線量当量 | Sv | rem |
|------|----|-----|
| 1    | 1  | 100 |
| 0.01 |    | 1   |